




Towards Accelerating Real-Time Path Tracing with Foveated Framework

Bipul Mohanto^{†1}, Sven Kluge¹, and Oliver Stadt¹

¹University of Rostock, Institute of Visual and Analytic Computing, Germany

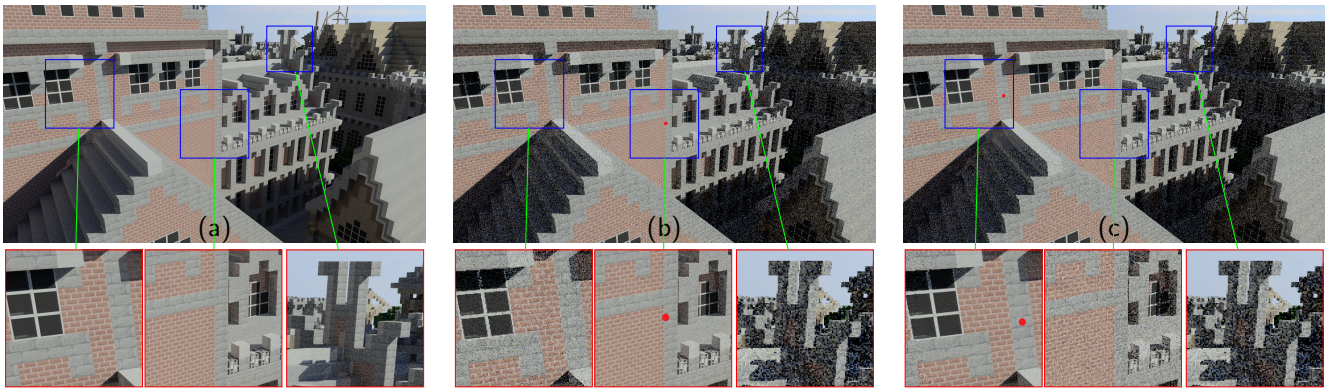


Figure 1: The output frames of our proposed foveated path tracing framework employing (a) uniform 32 samples per pixel across the Rungholt scene, rendered on average 0.37 fps. (b)–(c) Foveated sample numbers 32, 16, and 8 being used with selective lower resolution (Section 3) towards the periphery to reach an average framerate of 8.52 fps. (b) The fixation is at the center of the screen (indicated in red) and (c) at the top-left side of the screen (labeled in red). We achieved an outstanding, exceeding 22 \times speed up the rendering performance for the Rungholt scene (over 6.7 million triangles) at a 4K resolution. The selected areas are 2 \times zoomed in for better visualization.

Abstract

Path tracing is one of the most widespread rendering techniques for high-end graphics fidelity. However, the slow convergence time and presence of intensive noises make it infeasible for numerous real-time applications where physically corrected photo-realistic effects are salient. Additionally, the increased demand for pixel density, geometric complexity, advanced material, and multiple lights hinder the algorithm from attaining an interactive frame rate for real-time applications. To address these issues, we developed a framework to accelerate path tracing through foveated rendering, a robust technique that leverages human vision. Our dynamic foveated path-tracing framework integrates fixation data and selectively lowers the rendering resolution towards the periphery. The framework is built on NVIDIA’s OptiX 7.5 API with CUDA 12.1, serving as the base of future foveated path tracing research. Through comprehensive experimentation, we demonstrated the effectiveness of our framework in this paper. Depending on the scene complexity, our solution can significantly enhance rendering performance up to a factor of 25 without any notable visual differences. We further evaluated the framework using a structured error map algorithm with variable sample numbers and foveated area size.

CCS Concepts

• **Computing methodologies** \rightarrow **Ray tracing; Perception;**

1. Introduction

Path tracing [Kaj86] uses the sophisticated Monte Carlo estimation to approximate the behavior of light as it interacts with objects in the virtual environment. It is a powerful rendering technique for

[†] bipul.mohanto@uni-rostock.de

achieving several physically correct photorealistic effects, such as global illumination, soft shadows, caustics, color bleeding, reflections, refractions, and diffuse inter-reflections. These effects were previously elusive with rasterization techniques. Over the years, path tracing has been the dominant technique in mainstream offline renderings like movies, architecture visualization, and product designing. However, the convergence rate of path tracing is comparatively slow, $\mathcal{O}(1/\sqrt{n})$, where n is the number of samples [RWM*15]. Due to this slow convergence rate, noise is often visible in the final image with a low sample count. Therefore, denoising requires a large sample number for compelling photorealistic results. In fact, cutting the noise into half requires quadrupling the sample number [KIV*18]. This might seem effortless to offline rendering, but it is challenging in real-time rendering, especially with the current consume-grade hardware. Consequently, using path tracing in real-time applications such as games and interactive simulations is limited.

Besides the low sample count and noisy output, more research challenges must be addressed carefully to enable real-time path tracing. The plausible photorealistic effects require high ray traversal, tracing individual rays through complex scenes with numerous objects and surface intersections. Moreover, the complexity increases exponentially with each additional bounce. These can lead to another substantial overhead in achieving a real-time frame rate.

As technology advances, there is an increasing demand for displays with higher pixel density and refresh rates. For example, commercially used virtual reality headsets currently have an average angular resolution of 35 cycles per degree and a refresh rate of approximately 90 Hz [TLZ*18]. In contrast, humans can detect up to 60 cycles per degree in the fovea centralis [SCMP19]. To achieve a fully immersive experience replicating human vision, we require pixel density that is 6-10 times higher and refresh rates that are 10-20 times faster [CCK18]. These will further constrain path tracing as a practical solution for real-time applications.

Despite the limitations, we already have practical solutions to optimize real-time path tracing performance. Nonetheless, the solutions are primarily modern graphics hardware-dependent, such as robust data acceleration structures like bounding volume hierarchy [MOB*21]) or better ray-polygon intersection [PCPM23]. Apart from the hardware-based solutions, the foveated rendering is a hardware-independent graphics optimization technique that exploits human vision limitations (Section 2.1) to lower the rendering load without noticing any perceivable visual difference.

Although foveated rendering is more suitable for single-view displays with a wider field of view, multi-tiled display walls or even single desktops can equivalently take advantage to lower the extensive rendering load of real-time path tracing. For instance, while viewing from a 60 centimeters distance, an average human thumbnail at arm's length is equivalent to $1.5^\circ - 2^\circ$ which covers only 3% of a 21-inch display [DD17]. This visual angle is similar to the foveal angle. In addition, humans constantly perform saccades that scan and explore the scene to create a sharp image [GC21]. Therefore, uniformly rendering the entire scene is unnecessary, and foveated rendering can be an efficient solution with limited hardware capacity. In fact, an average human can only perceive

roughly 8% of a 60° desktop monitor with the highest graphics fidelity [WS19].

Foveated rendering has traditionally utilized rasterization technology, which is widely employed throughout computer graphics. Over the years, numerous foveated rendering algorithms have been developed, primarily based on the rasterization pipeline. In a recent survey, Mohanto et al. [MIGS22] categorized these methods into four categories: adaptive resolution, geometry simplification, shading and chromatic degradation, and spatiotemporal deterioration. However, there has been a gradual transition towards ray tracing due to advancements in graphics hardware and the demand for physically accurate global features. Unlike rasterization, ray tracing (path tracing is a subset of ray tracing) offers better flexibility for per-pixel manipulation in foveated rendering [KIV*18]. Additionally, Koskela et al. [KVJT16] estimated that around 94% rays can be disregarded with foveated rendering, making path tracing even faster.

Recently, Calla et al. [RMPS23] published a foveated path tracing framework for multi-tiled display walls, which motivated us to develop a better and more flexible framework. Unlike their framework, which only reduces shading load, our study decreased both the rendering resolution and shading load. Additionally, while the authors used a per-pixel approach for the periphery, we utilized a per-pixel block approach. Our framework used 8 samples per (4×4) pixels' block in the periphery, whereas their framework could only lower the sample number to 1. Our framework achieved better visual quality and accelerated the frame rate by over 25 times, while the authors claimed an acceleration by a factor of 4.45.

The main contributions to this article can be summarized as follows. We present a foveated framework based on NVIDIA OptiX and CUDA that allows real-time path tracing on geometry-intensive complex scenes at a 4K resolution. Using foveated path tracing, we can significantly improve the rendering performance. Unlike rendering the entire scene in a per-pixel approach, our framework only renders the foveated area with a per-pixel approach. It divides the rest of the screen space into two other subregions and renders in a $(n \times n)$, and $(m \times m)$ pixel-block manner (see Section 3). The pixel block size and sampling numbers are user-defined. Users can input different numbers to investigate the balance between performance and rendering quality.

2. Related work

Foveated rendering has garnered significant attention from graphics researchers since the seminal study by Guenter et al. [GFD*12]. According to a recent publication by Mohanto et al. [MIGS22] on page 475, there has been a decisive momentum in publication per year. Weier et al. [WSR*17] conducted the first survey on foveated rendering and further elaborated in his thesis [Wei19]. Besides, Koskela et al. [KVJT16] conducted a survey report solely focused on foveated path tracing. In 2022, Mohanto et al. [MIGS22] published the first in-depth survey on existing foveated rendering algorithms. Likewise, Jabbireddy et al. [JSMV22] presented a foveated rendering taxonomy and Wang et al. [WSL23] published an overview of the latest foveated rendering algorithms. Similarly, Singh et al. [SHL*23] focused on a study on possible power consumption and optimization through foveated rendering.

For the past three decades, rasterization has been the most popular technique for foveated rendering [MIGS22]. However, there has been a recent shift towards ray tracing [Whi05]. Although foveated ray tracing was initially utilized for large tiled-display walls [WMR*14], recent works have focused on single view head-mounted displays (HMDs) [FH14; WRK*16; VKI*18; SCMP19; YLC20; KKI21], which are considered the optimal choice for foveated rendering. Fujita and Harada [FH14] were among the first to adopt the foveated sampling pattern using a k-nearest neighbor filter. However, the mathematical model did not take into account the actual contrast sensitivity function. Similarly, Siekawa et al. [SCMP19] proposed a sparse sampling mask to reduce the primary rays from the gaze point, while Weier et al. [WRK*16] reused foveated temporal data from the previous frame.

There have been several recent studies conducted on foveated ray tracing. One such study by Peuhkurinen and Mikkonen [PM21] utilized a foveated log-polar space to reduce the number of rays. Another study by Yang et al. [YLC20] introduced a variable rate sampling policy, while Kim et al. [KKI21] proposed a perceptual sampling technique using adaptive supersampling. Additionally, Dahlin and Sundstedt [DS21] combined variable rate shading [NVI19] and inline ray tracing to create superior reflections at a quarter of the native resolution, which is widely used in the gaming industry.

In recent years, foveated path tracing has emerged as an alternative to traditional ray tracing methods. However, this technique remains a challenging task, with limited research available. Previous studies have primarily focused on large display-tiled walls [RWM*15]. More recently, Koskela et al. [KIV*18; KLM*19] have made significant strides in the field, pioneering foveated path tracing on HMD. Their work includes the first foveated path tracing preview system (2018) [KIV*18] and log-polar space mapping for ray generation (2019) [KLM*19], which have garnered significant attention. Additionally, Lotvonen et al. (2020) [LKJ20] explored the potential application of machine learning methods for foveated path tracing denoising, another promising contribution. Most recently, Kim and Sung (2021) [KS21] designed the first foveated path tracing framework tailored explicitly for smartphone-based virtual reality displays. Polychronakis et al. [PKM21] presented a foveated path tracing sandbox for determining the eccentricity angle threshold. However, the sandbox could not work on real-time path tracing and emulated foveated rendering as post-processing. Besides, a minimum of 1 sample could be applied in the sandbox. Likewise, Calla et al. [RMPS23] developed a foveated path tracing framework for multi-tiled large display walls that reduces the required peripheral sample number to a minimum of 1 per pixel.

2.1. Physiology of human eye and vision

Human vision is arguably the most complex of all biological senses. The visual process begins with the eye and ends at the visual cortex at the back of the brain [Jou17]. The pupil allows light from the environment to enter the eye, which is then focused by the cornea and lens to create sharp images of the objects on the retina [GC21]. However, due to the uneven photoreceptor distribution over the retina, humans cannot retain the same level of sharpness throughout their entire field of view.

Human has two types of photoreceptors: rods and cones. Rods are brightness sensitive under scotopic vision, while cones are color sensitive under photopic vision [BS10]. There are approximately 6 million cones in the retina; nevertheless, they are only densely packed in the central region, about 5.2° from the visual axis [GC21]. This region, known as the fovea, roughly covers 1.5 mm in diameter in the retina [SEB03]. Due to these dense cone cells, foveal vision is only fine-grained with the highest visual acuity. Through the parafovea ($5.2^\circ - 9^\circ$) and perifovea ($9^\circ - 17^\circ$), cone density decreases rapidly, and rod density increases greatly [And02].

There are around 20 times more rods than the cones [GC21], but its maximum density is close to 20° from the visual axis [Ost35]. That makes the peripheral vision more sensitive to luminance than chrominance. At the same time, it makes the foveated rendering process even more challenging as flickers are easily noticeable in this region [KpYK19]. To minimize the flickering effect, filters like Gaussian are trendy. However, loss of local brightness will further create a tunnel vision effect [PSK*16].

3. The rendering framework

We designed a heuristic desktop-based prototype where the foveated path tracing delivers significant interactive performance for large complex scenes with global illumination effects. Users have the option to select either uniform or foveated path tracing modes at the outset. While both modes allow for the adjustment of the sample number, in foveated mode, users can also adjust the size of the fovea and intermediate regions. By utilizing the foveated mode, the framework only renders the foveated region at the native resolution, significantly reducing the rendering load by employing a pixel-block approach for the intermediate and peripheral regions. Furthermore, the user can customize the block size, just like variable rate shading. [NVI19]. Lastly, the three regions are blended seamlessly with just one render pass. Please refer to Figure 2 for a visual representation of these processes. The upcoming sections will provide a detailed explanation of these steps.

3.1. Area of interest

At the beginning of the pipeline (Figure 2. a), we determine the area of interest and separate the rendering layers. Studies have suggested different numbers of regions. There are two [SCM15; CC16], three [GFD*12; FGS13; Mar18], and even six [GP98] layers have been proposed in literature. However, we have utilized the commonly used three-layer model for this framework. We begin by extracting the fixations in Cartesian space to determine the three consecutive regions and then calculate the Euclidean distance for each pixel. It is worth noting that we currently employ predefined pseudo-fixations, as we do not possess a real eye tracker. Nonetheless, we can expand the framework with one in the future. Moreover, the fixations are further forwarded to the device side in real-time to control the ray generation routine described in section 3.2. To match the highest visual acuity of humans, we exploited the *tangent* formula [Mat97] to convert the cycles per degree into pixels per degree. From the simple geometry, the display portion is covered by the visual angle:

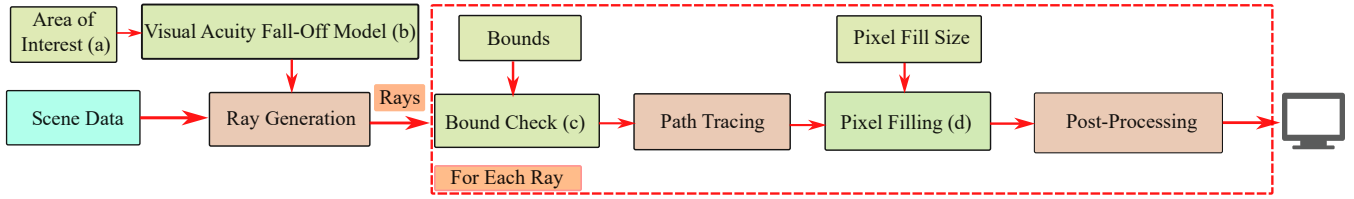


Figure 2: Pipeline of our proposed foveated path tracing framework. Based on the fixations, (a) the framework first defines the Area of Interest, (b) followed by the visual acuity fall-off model, and (c) bound check to control ray numbers over the scene. After the ray propagation over the scene, we adopted (d) pixel filling to fill out the missing pixels. The framework displays the final results on the screen after the post-processing is completed.

$$a = 2 \cdot d \cdot \tan \frac{e}{2}, \quad (1)$$

$$r = \frac{a \cdot R}{A}. \quad (2)$$

Where e is the eccentricity angle in degrees, and d is the distance from the eye in centimeters. r is the radius in pixel number, A is the display dimension in pixels, and R is the display size in centimeters. It is important to note that both a and A should be in the same direction, either in width or height. We can see that equation 1 is distance-dependent; we used 60 cm in our framework. Our display has a 4k resolution with an area of (70.848×39.852) square centimeters. According to equation 2, the approximate values for the foveated and intermediate radii are 147 and 482 pixels, respectively. These radii further determine the area of interest (AoI) mentioned in Figure 2 (a).

3.2. Piecewise visual acuity fall-off model

The second part of the pipeline is the visual acuity fall-off model (Figure 2. b). When it comes to generating a foveated sampling pattern, there are three main visual acuity fall-off models discussed in the literature: piecewise [YLC20], linear [WRK*16], and quadric [KIV*18]. Out of these, the quadric model is considered the most accurate as it is based on psychophysical experiments and closely resembles human visual acuity. However, we have used the piecewise visual acuity fall-off model due to its simplicity. Our piecewise model follows the widely accepted sample distribution ratio of 1, $\frac{1}{2}$, and $\frac{1}{4}$ in foveated rendering, as suggested by seminal studies such as Levoy (1991) [LW90] and Guenter (2012) [GFD*12].

In order to achieve realistic results, path tracing typically requires a high number of samples. However, in the realm of real-time rendering, we must balance visual quality with frame rate. According to a study by Weier et al., [WRK*16], using 16 or more samples per pixel is appropriate for real-time ray tracing. Additionally, Fujita and Harada [FH14] suggest that to prevent visual artifacts real-time ray tracing applications should use at least 32 samples per pixel. Therefore, we have adopted 32 samples per pixel as the consistent sample count and utilized the piecewise sampling ratio to determine the foveated sample count:

$$f(e) = \begin{cases} \tau_1 / px, & \text{if } e \leq e_f, & (3a) \\ \tau_2 / (n \times n) px, & \text{elif } e_f < e \leq e_i, & (3b) \\ \tau_3 / (m \times m) px, & \text{otherwise.} & (3c) \end{cases}$$

The samples (τ_1, τ_2, τ_3) propagate according to the eccentricity angle (e) with equation 1. For our purpose, e_f is the foveated angle, 5.2° [GFD*12; PSK*16], and e_i is the intermediate angle, 17° [RWH*17]. Here, n and m are the pixel numbers that create a block and can be user-defined. We used $n = 2$ and $m = 4$ for our framework. From the equations 3a–3c, we cast 32 samples (τ_1) per pixel for the foveated region, 16 samples (τ_2) per (2×2) pixel block for the intermediate region, and 8 samples (τ_3) for (4×4) pixel blocks in the periphery region. Finally, we blend the three regions under one single rendering pass. A visual model is presented in Figure 3.

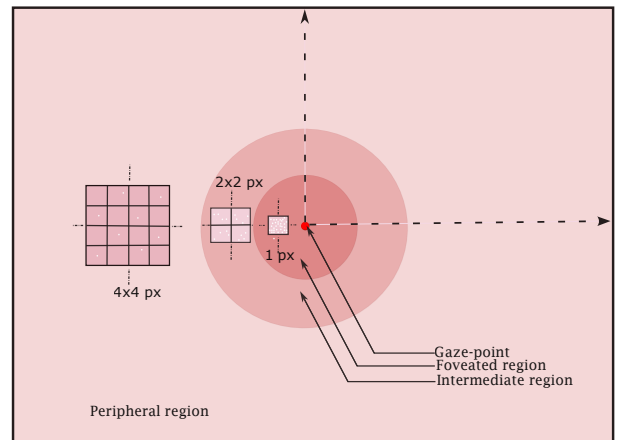


Figure 3: Visual illustration of the sample distribution across the scene. We applied three distinct policies for the sample cast from equation 3a–3c. The innermost circle (foveated region) casts 32 samples per pixel, the intermediate area casts 16 samples for (2×2) pixel block, and the outermost periphery area casts 8 samples per (4×4) pixel block.

3.3. Bound check and path tracing

The third part of our pipeline is the bound check (Figure 2. c) Before casting any primary ray, we check its initial position in screen

space against the boundaries of the radii of its region. The bound check is simply a binary operation. If the ray does not meet the bounds check, we discard it immediately. Otherwise, we keep the ray for further ray propagation.

The backward path tracing [Kaj86] is the backbone of our framework. The variable sample numbers are further distributed according to multiple importance sampling [Vea98] for better light effects. As surface appearance is of utmost importance for photorealistic outputs, we employed the Disney Bidirectional Reflectance Distribution Function (BRDF) [BS12] as the lighting model. Although the model is not fully physically corrected (disobeying energy conservation), it serves our current purpose. We limited the recursion depth to 3 in the scene to avoid further computation load but allow global illumination. In addition, our path tracer supports ambient light and environmental light as an illumination source.

3.4. Pixel filling and post-processing

The final aspect of our framework is the pixel-filling step (shown in Figure 2. d). As we cast fewer rays than the actual pixel number, the missing pixels are filled with the respective pixel block of the scene using standard linear interpolation. Moreover, we can activate/deactivate the final color accumulation. However, there is little scope for accumulation in a real-time application with constant eye movements. Therefore, we presented the data (Figure 1, 4, 7) in this study without accumulation. We applied subpixel jitter, exposure compensation, and Reinhard tone mapping [SbMMS12] during post-processing for a mellow output.

In the given framework, the GPU plays a crucial role in executing the ray generation, intersection, closest hit, and miss programs (shaders referred to as “programs” in the OptiX ecosystem). It should be noted that the any hit shader has not been incorporated at present. Since the OptiX API and underlying CUDA lack native support for image display, we have leveraged CUDA-OpenGL interoperability and the open-source GLFW library to showcase the final images from CUDA Buffers directly.

3.5. Framework setup

The framework is developed with OptiX 7.5 API [PBD*10] with CUDA 12.1. It can easily be adapted to newer versions of OptiX with just minor modifications. For our hardware, we utilized an Intel Core i9 12900Ks processor with 128 GBytes of DDR5 RAM. Our system has an NVIDIA GeForce RTX 3090 GPU with 24 Gbytes VRAM. We used the latest NVidia studio driver, 536.99. Our framework has been tested on Windows 10 Education 22H2 ($\times 64$) and can also be executed on the Linux platform. To visualize the final outputs, we used a Dell G3223Q 32-inch 4K UHD Gaming Monitor with a density of 54 pixels per cm.

4. Results and discussion

In this section, we share the results of our dynamic foveated path tracing framework by evaluating the rendering techniques on three geometry-intensive scenes: Crytek Sponza, Lost Empire, and San Miguel 2.0 [McG17]. Noteworthy, we do not have an eye tracker,

and the framework relies on predefined pseudo fixations. However, it can be easily extended with a real-time eye tracker. Table 1 presents the triangle count, frame rate, and performance comparison with the setup mentioned in the previous section 3.5. On the other hand, Figure 5 shows the three scenes’ rendering time in uniform and foveated path tracing methods. We calculated the frame rate and rendering time with a fixed pathway movement and 199 consecutive frames.

Table 1: *The following table provides in-depth details about three rendered scenes (1st column) and their respective outcomes. The 2nd column presents the total number of triangles, and the 3rd column shows the average frame rate with 32 samples over the entire scene. The 4th column displays the resulting average frame rates with 32, 16, and 8 sample numbers, respectively. The 5th column exhibits the speed-up that our framework achieved.*

Scene	Triangles	fps (uni)	fps (fov)	Speed-up (\times)
Lost Empire	224,998	0.42	10.20	23.29
Crytek Sponza	262,267	0.24	7.48	30.17
San Miguel 2.0	9,980,699	0.23	5.71	23.83

The test results show that without foveation, Lost Empire, Crytek Sponza, and San Miguel 2.0 have an average frame rate of 0.42, 0.24, and 0.23 fps, respectively. With foveation, there is an incredible performance improvement in average frame rate, 10.20, 7.48, and 5.70 fps, which is more than 25 times performance boost on average. Additionally, the rendering time of 199 consecutive frames is illustrated in Figure 5. It is without a doubt that the rendering time is proportional to the scene complexity. The foveated sampling lowers the rendering time in a similar pattern but with much less time. The final outputs are presented in Figure 4. Without any denoising algorithm, the outputs with lower sampling numbers are naturally more noisy. However, the outer boundaries are hardly noticeable, and the degradation quality is less destructive with frequent gaze movements.

Applying a more aggressive foveation area and/or sample number can further improve the rendering performance. For instance, reducing the foveated and intermediate areas in half on the Crytek Sponza scene while maintaining the same foveated sample number and pixel-block approach can speed up the rendering process by 44.67 times. This is a significant improvement from the current setup, which increased rendering by 30.17 times (see Table 1, column 5). The frame rate can improve approximately 1.48 times by halving the foveated and intermediate areas. Moreover, reducing the sample number also significantly affects rendering speed. We tested various sample number configurations on the Crytek Sponza scene to compare performance differences. Table 2 indicates that the frame rate increases linearly with the lower sampling number. We have also included a rendering time visualization for the same 199 successive frames in Figure 6.

Despite its potential benefits, aggressive foveation carries significant risks. It may lead to a noticeable decrease in graphics quality in the outer regions, particularly in applications like virtual reality, where it can disrupt the immersive experience. Besides, we further evaluated the different sampling combinations with the latest



Figure 4: Visual comparison between uniform and foveated path tracing. We applied 32 samples per pixel (top row) in uniform path tracing. Contrarily, in foveated path tracing (bottom row), we employed 32 samples per pixel for foveated, 16 samples per (2×2) pixel block for intermediate, and 8 samples per (4×4) pixel block in the periphery area. We selected three triangle-intensive scenes for evaluation: Crytek Sponza (a, d), Lost Empire (b, e), and San Miguel 2.0 (c, f). Note: The frames are displayed without accumulation. The fixations are marked with red at the bottom row.

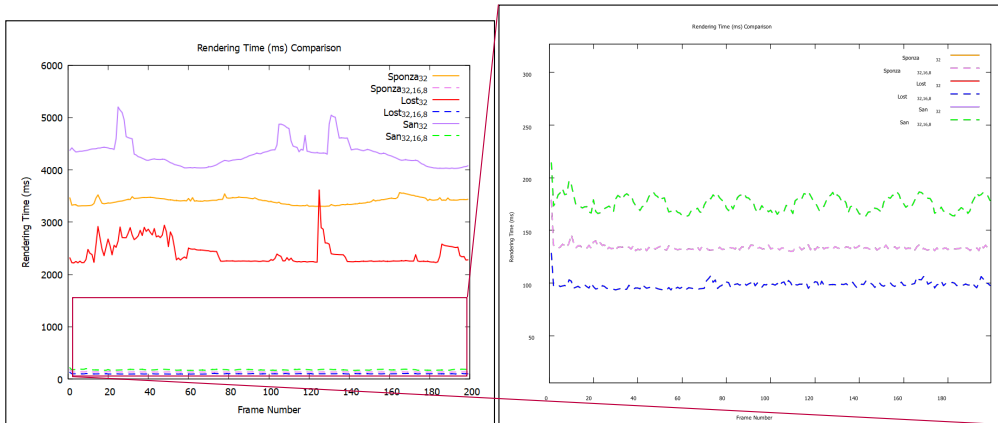


Figure 5: The rendering time comparison over 199 successive frames of Lost Empire (Lost), Crytek Sponza (Sponza), and San Miguel 2.0 (San) scenes. Rendering with uniform 32 samples is marked with a solid line, and foveated sampling is marked with broken lines. The right figure zooms in on the foveated rendering time for improved clarity.

structured error map algorithm, FLIP [ANA*20]. FLIP focuses on evaluating differences between rendered images and ground truths. The algorithm generates a map that approximates the perceptual difference between two images. Figure 7 illustrates the perceptual difference between different sampling combinations employed in Table 2. In the bottom row, the foveated sample areas are highlighted with black, which means no visual differences concerning the reference image; the peripheral areas are gradually highlighted in yellow, representing perceptual errors.

Due to the slow convergence time and high noise level, real-time path tracing for a complex scene on a pixel-intensive display

is still infeasible. In this study, we admitted these issues and presented a dynamic foveated path tracing implementation with complex scenes on a 4K display. We have demonstrated that our framework can significantly accelerate the real-time path tracing performance. The results are sufficiently pleasing with such a small variable sample number (Figure 4) since we did not employ any additional denoising. The graphics degradation is hardly noticeable under a static head position with real-time eye movement.

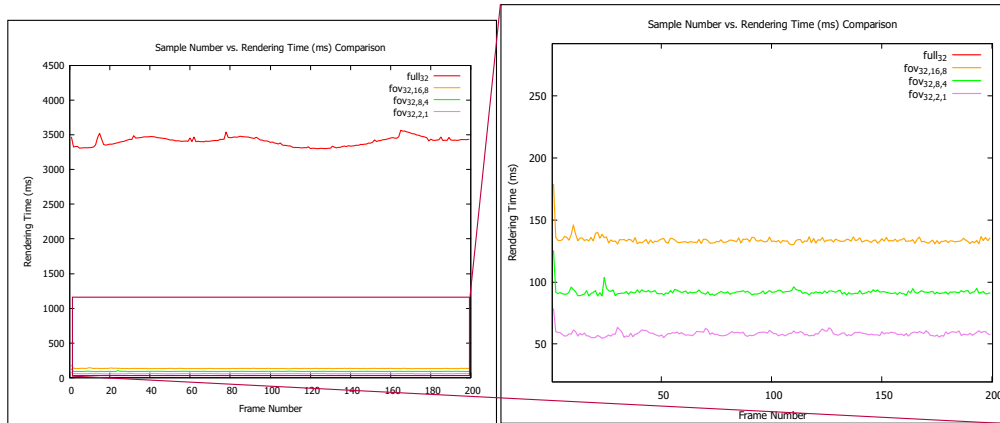


Figure 6: The rendering time comparison between different sample number combinations over 199 consecutive frames on Crytek Sponza scene. The right figure zooms in on the foveated rendering time for improved clarity.

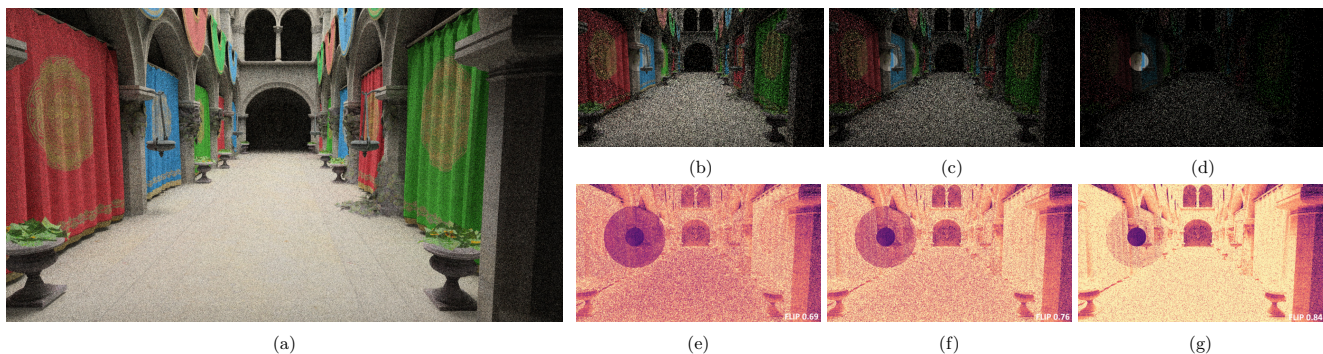


Figure 7: Visual outputs from the Crytek Sponza scene with different sample number configurations. (a) uniform path tracing with 32 samples per pixel, Figure (b)–(d) the foveated sample number kept constant as 32 samples per pixel, intermediate and periphery was varied (16,8), (8,4), and (2,1). Figure (e)–(g) is the FLIP error map with the reference image (a). Here, black indicates imperceptible error, while yellow represents high visual error. Moreover, the fewer highlighted area indicates better visual quality [ANA*20].

Table 2: This study measures the speed-up of Crytek Sponza scene using different sampling configurations. The configurations are applied only in the intermediate (Int.) and periphery (Peri.) regions and compared to uniform path tracing with 32 sample numbers.

Scene	Sample configurations			fps	Speed-up (\times)
	Fovea	Inter.	Peri.		
Crytek Sponza	32	–	–	0.30	–
	32	16	8	7.48	23.93
	32	8	4	10.90	35.33
	32	2	1	17.14	56.13

5. Conclusion and future work

In this work, we presented a novel foveated framework that employs the variable sampling number and pixel-block rendering approach to improve the performance of real-time path tracing. This framework can meet the high computational demands of path tracer on a pixel-intensive display and provides an efficient, flexible, and

practical solution. Our research has shown minimal visual differences outside the fovea, and we anticipate that using a real eye-tracker will help prevent any visible degradation in graphics quality for the viewer. This framework could serve as a sturdy foundation for future research on foveated path tracing.

Although our results are promising, the framework still has some limitations we plan to address in future investigations. We have noticed some performance disparities in our current implementation that could be due to hardware architecture. Not all rays are being discarded during the bounds check, hindering our efforts to improve performance. In fact, the ray generation process is initiated separately for each pixel within a rectangular area. However, we require circular foveated and peripheral regions, so rays outside the circle bound are being discarded. To speed up the computation process, the graphics hardware splits the rays into smaller sections that can be processed in parallel. Nonetheless, the processing time remains unchanged even if some of the rays in a section are discarded due to a bounds check. We are seeking a better solution to optimize the bounds check by only generating rays for pixels

within the bounds. This will be beneficial in enhancing efficiency for upcoming tasks.

Finally, our framework is limited to the piecewise visual acuity fall-off model [YLC20]. To overcome this, we plan on exploring other models such as the linear [WRK*16] and quadric [KIV*18] visual acuity fall-off models. This will support us to define a better sample distribution. To conduct a user study, we aim to replace the existing cursor-based pseudo-fixation points with an eye tracker. This will assist us to find the flaws in the current framework. Additionally, reducing the sample number has introduced some additional noises that need to be addressed separately for optimal results. We intend to explore the popular denoising options available in the literature, such as OptiX AI denoiser [CKS*17] and foveated denoiser [WAF*21; MK21].

Acknowledgments

The authors would like to sincerely thank the 3D scene creators used during testing, Frank Meinel (Crytek Sponza), Morgan McGuire (Lost Empire), Guillermo M. Leal Llaguno (San Miguel 2.0), and Kescha (Rungholt). Additionally, the authors would also like to extend their gratitude to Poly Heaven for generously providing their HDRI lighting assets. Their contribution proved to be incredibly beneficial throughout our research project.

References

- [ANA*20] ANDERSSON, PONTUS, NILSSON, JIM, AKENINE-MÖLLER, TOMAS, et al. “FLIP: A Difference Evaluator for Alternating Images”. *Proc. ACM Comput. Graph. Interact. Tech.* 3.2 (Aug. 2020). DOI: [10.1145/3406183](https://doi.org/10.1145/3406183). URL: <https://doi.org/10.1145/3406183> 6, 7.
- [And02] ANDERSEN, SIGURD RY. “The history of the Ophthalmological Society of Copenhagen 1900–50”. *Acta Ophthalmologica Scandinavica* 80 (2002), 6–17 3.
- [BS10] BARBUR, JL and STOCKMAN, A. “Photopic, mesopic and scotopic vision and changes in visual performance”. *Encyclopedia of the Eye* 3 (2010), 323–331 3.
- [BS12] BURLEY, BRENT and STUDIOS, WALT DISNEY ANIMATION. “Physically-based shading at disney”. *Acm Siggraph*. Vol. 2012. 2012. 2012, 1–7 5.
- [CC16] CUERVO, EDUARDO and CHU, DAVID. “Poster: Mobile Virtual Reality for Head-Mounted Displays With Interactive Streaming Video and Likelihood-Based Foveation”. *Proceedings of the 14th Annual International Conference on Mobile Systems, Applications, and Services Companion*. MobiSys ’16 Companion. Singapore, Singapore: Association for Computing Machinery, 2016, 130. ISBN: 9781450344166. DOI: [10.1145/2938559.2938608](https://doi.org/10.1145/2938559.2938608). URL: <https://doi.org/10.1145/2938559.2938608> 3.
- [CCK18] CUERVO, EDUARDO, CHINTALAPUDI, KRISHNA, and KOTARU, MANIKANTA. “Creating the Perfect Illusion: What Will It Take to Create Life-Like Virtual Reality Headsets?”. *Proceedings of the 19th International Workshop on Mobile Computing Systems & Applications*. HotMobile ’18. Tempe, Arizona, USA: Association for Computing Machinery, 2018, 7–12. ISBN: 9781450356305. DOI: [10.1145/3177102.3177115](https://doi.org/10.1145/3177102.3177115). URL: <https://doi.org/10.1145/3177102.3177115> 2.
- [CKS*17] CHAITANYA, CHAKRAVARTY R. ALLA, KAPLAYAN, ANTON S., SCHIED, CHRISTOPH, et al. “Interactive Reconstruction of Monte Carlo Image Sequences Using a Recurrent Denoising Autoencoder”. *ACM Trans. Graph.* 36.4 (July 2017). ISSN: 0730-0301. DOI: [10.1145/3072959.3073601](https://doi.org/10.1145/3072959.3073601). URL: <https://doi.org/10.1145/3072959.3073601> 8.
- [DD17] DUCHOWSKI, ANDREW T and DUCHOWSKI, ANDREW T. *Eye tracking methodology: Theory and practice*. Springer, 2017 2.
- [DS21] DAHLIN, ALEXANDER and SUNDSTEDT, VERONICA. “Improving Ray Tracing Performance with Variable Rate Shading”. *Computer Graphics and Visual Computing (CGVC)*. Ed. by XU, KAI and TURNER, MARTIN. The Eurographics Association, 2021. ISBN: 978-3-03868-158-8. DOI: [10.2312/cgvc.202113193](https://doi.org/10.2312/cgvc.202113193).
- [FGS13] FINCH, MARK, GUENTER, BRIAN, and SNYDER, JOHN. “Foveated 3D display”. *ACM SIGGRAPH 2013 emerging technologies*. 2013, 1–1 3.
- [FH14] FUJITA, MASAHIRO and HARADA, TAKAHIRO. “Foveated real-time ray tracing for virtual reality headset”. *Light Transport Entertainment Research* (2014) 3, 4.
- [GC21] GOLDSTEIN, E BRUCE and CACCIAMANI, LAURA. *Sensation and perception*. Cengage Learning, 2021 2, 3.
- [GFD*12] GUENTER, BRIAN, FINCH, MARK, DRUCKER, STEVEN, et al. “Foveated 3D Graphics”. *ACM Trans. Graph.* 31.6 (Nov. 2012). ISSN: 0730-0301. DOI: [10.1145/2366145.2366183](https://doi.org/10.1145/2366145.2366183). URL: <https://doi.org/10.1145/2366145.2366183> 2–4.
- [GP98] GEISLER, WILSON S. and PERRY, JEFFREY S. “A real-time foveated multiresolution system for low-bandwidth video communication”. Vol. 3299. Cited by: 334. 1998, 294–305. DOI: [10.1117/12.320120](https://www.scopus.com/inward/record.uri?eid=2-s2.0-85026149763&doi=10.1117%2F12.320120&partnerID=40&md5=f709ec2b0c08b8310c566d2286550dcd3). URL: <https://www.scopus.com/inward/record.uri?eid=2-s2.0-85026149763&doi=10.1117%2F12.320120&partnerID=40&md5=f709ec2b0c08b8310c566d2286550dcd3>.
- [Jou17] JOUKAL, MAREK. “Anatomy of the human visual pathway”. *Homonymous visual field defects* (2017), 1–16 3.
- [JSMV22] JABBIREDDY, SUSMIJA, SUN, XUETONG, MENG, XIAOXU, and VARSHNEY, AMITABH. *Foveated Rendering: Motivation, Taxonomy, and Research Directions*. 2022. arXiv: 2205.04529 [cs.GR] 2.
- [Kaj86] KAJIYA, JAMES T. “The Rendering Equation”. *SIGGRAPH Comput. Graph.* 20.4 (Aug. 1986), 143–150. ISSN: 0097-8930. DOI: [10.1145/15886.15902](https://doi.org/10.1145/15886.15902). URL: <https://doi.org/10.1145/15886.15902> 1, 5.
- [KIV*18] KOSKELA, MATIAS K., IMMONEN, KALLE V., VIITANEN, TIMO T., et al. “Instantaneous foveated preview for progressive Monte Carlo rendering”. *Computational Visual Media* 4.3 (2018), 267–276. DOI: [10.1007/s41095-018-0113-0](https://www.scopen.com/article/10.1007/s41095-018-0113-0). URL: <https://www.scopen.com/article/10.1007/s41095-018-0113-0> 2–4, 8.
- [KKI21] KIM, YOUNGWOOK, KO, YUNMIN, and IHM, INSUNG. “Selective Foveated Ray Tracing for Head-Mounted Displays”. *2021 IEEE International Symposium on Mixed and Augmented Reality (ISMAR)*. 2021, 413–421. DOI: [10.1109/ISMAR52148.2021.000583](https://doi.org/10.1109/ISMAR52148.2021.000583).
- [KLM*19] KOSKELA, MATIAS, LOTVONEN, ATRO, MÄKITALO, MARKKU, et al. “Foveated Real-Time Path Tracing in Visual-Polar Space”. *Eurographics Symposium on Rendering - DL-only and Industry Track*. Ed. by BOUBEKEUR, TAMY and SEN, PRADEEP. The Eurographics Association, 2019. ISBN: 978-3-03868-095-6. DOI: [10.2312/sr.201912193](https://doi.org/10.2312/sr.201912193).
- [KpYK19] KWONOH-SEOK, PARKKEON-KUK, YOONJOSEPH, and KIMYOUNG-BONG. “Fast Ray Reordering and Approximate Sibson Interpolation for Foveated Rendering on GPU”. *Journal of Korea Multimedia Society* 22.2 (Feb. 2019), 311–321 3.
- [KS21] KIM, SEONG KI and SUNG, MAN KYU. “Efficient Path Tracer for the Presence of Mobile Virtual Reality”. *Hum.-Cent. Comput. Inf. Sci* 11 (2021), 1–14 3.
- [KVJT16] KOSKELA, MATIAS, VIITANEN, TIMO, JÄÄSKELÄINEN, PEKKA, and TAKALA, JARMO. “Foveated Path Tracing”. *Advances in Visual Computing*. Ed. by BEBIS, GEORGE, BOYLE, RICHARD, PARVIN, BAHRAM, et al. Cham: Springer International Publishing, 2016, 723–732. ISBN: 978-3-319-50835-1 2.

- [LKJ20] LOTVONEN., ATRO, KOSKELA., MATIAS, and JÄÄSKELÄINEN., PEKKA. “Machine Learning is the Solution Also for Foveated Path Tracing Reconstruction”. *Proceedings of the 15th International Joint Conference on Computer Vision, Imaging and Computer Graphics Theory and Applications (VISIGRAPP 2020) - GRAPP*. INSTICC. SciTePress, 2020, 361–367. ISBN: 978-989-758-402-2. DOI: [10.5220/00091563036103673](https://doi.org/10.5220/00091563036103673).
- [LW90] LEVOY, MARC and WHITAKER, ROSS. “Gaze-Directed Volume Rendering”. *SIGGRAPH Comput. Graph.* 24.2 (Feb. 1990), 217–223. ISSN: 0097-8930. DOI: [10.1145/91394.91449](https://doi.org/10.1145/91394.91449). URL: <https://doi.org/10.1145/91394.914494>.
- [Mar18] MARIANOS, NIKOLAOS. “Foveated rendering algorithms using eye-tracking technology in virtual reality”. *Technical University of Crete* (2018) 3.
- [Mat97] MATKOVIC, KRESIMIR. “Tone mapping techniques and color image difference in global illumination”. PhD thesis. Matkovic, 1997 3.
- [McG17] MCGUIRE, MORGAN. *Computer Graphics Archive*. <https://casual-effects.com/data>. July 2017. URL: <https://casual-effects.com/data5>.
- [MIGS22] MOHANTO, BIPUL, ISLAM, ABM TARIQUL, GOBBETTI, ENRICO, and STAADT, OLIVER. “An integrative view of foveated rendering”. *Computers & Graphics* 102 (2022), 474–501. ISSN: 0097-8493. DOI: <https://doi.org/10.1016/j.cag.2021.10.010>. URL: <https://www.sciencedirect.com/science/article/pii/S009784932100221123>.
- [MK21] MILEF, NICHOLAS and KALANTARI, NIMA. “Foveated Monte-Carlo Denoising”. *ACM SIGGRAPH 2021 Posters*. SIGGRAPH '21. Virtual Event, USA: Association for Computing Machinery, 2021. ISBN: 9781450383714. DOI: [10.1145/3450618.3469140](https://doi.org/10.1145/3450618.3469140). URL: <https://doi.org/10.1145/3450618.34691408>.
- [MOB*21] MEISTER, DANIEL, OGAKI, SHINJI, BENTHIN, CARSTEN, et al. “A Survey on Bounding Volume Hierarchies for Ray Tracing”. *Computer Graphics Forum* 40.2 (2021), 683–712. DOI: <https://doi.org/10.1111/cgf.142662>. eprint: <https://onlinelibrary.wiley.com/doi/pdf/10.1111/cgf.142662>. URL: <https://onlinelibrary.wiley.com/doi/abs/10.1111/cgf.1426622>.
- [NVI19] NVIDIA. *VRWorks - Variable Rate Shading (VRS)*. 2019. URL: <https://developer.nvidia.com/vrworks/graphics/variable-rateshading> (visited on 06/08/2023) 3.
- [Ost35] OSTERBERG, GUSTAV A. “Topography of the layer of rods and cones in the human retina”. *Acta ophthalmologica* (1935) 3.
- [PBD*10] PARKER, STEVEN G., BIGLER, JAMES, DIETRICH, ANDREAS, et al. “OptiX: A General Purpose Ray Tracing Engine”. *ACM Trans. Graph.* 29.4 (July 2010). ISSN: 0730-0301. DOI: [10.1145/1778765.1778803](https://doi.org/10.1145/1778765.1778803). URL: <https://doi.org/10.1145/1778765.17788035>.
- [PCPM23] PERES, VICTOR, CLUA, ESTEBAN, PORCINO, THIAGO, and MONTENEGRO, ANSELMO. “Non-homogeneous denoising for virtual reality in real-time path tracing rendering”. *Graphical Models* 129 (2023), 101184. ISSN: 1524-0703. DOI: <https://doi.org/10.1016/j.gmod.2023.101184>. URL: <https://www.sciencedirect.com/science/article/pii/S15240703230001402>.
- [PKM21] POLYCHRONAKIS, ANDREAS, KOULIERIS, GEORGE ALEX, and MANIA, KATERINA. “Emulating Foveated Path Tracing”. *Proceedings of the 14th ACM SIGGRAPH Conference on Motion, Interaction and Games*. MIG '21. Virtual Event, Switzerland: Association for Computing Machinery, 2021. ISBN: 9781450391313. DOI: [10.1145/3487983.3488295](https://doi.org/10.1145/3487983.3488295). URL: <https://doi.org/10.1145/3487983.34882953>.
- [PM21] PEUHKURINEN., ANTTI and MIKKONEN., TOMMI. “Real-time Human Eye Resolution Ray Tracing in Mixed Reality”. *Proceedings of the 16th International Joint Conference on Computer Vision, Imaging and Computer Graphics Theory and Applications (VISIGRAPP 2021) - GRAPP*. INSTICC. SciTePress, 2021, 169–176. ISBN: 978-989-758-488-6. DOI: [10.5220/00102057016901763](https://doi.org/10.5220/00102057016901763).
- [PSK*16] PATNEY, ANJUL, SALVI, MARCO, KIM, JOOHWAN, et al. “Towards Foveated Rendering for Gaze-Tracked Virtual Reality”. *ACM Trans. Graph.* 35.6 (Dec. 2016). ISSN: 0730-0301. DOI: [10.1145/2980179.2980246](https://doi.org/10.1145/2980179.2980246). URL: <https://doi.org/10.1145/2980179.298024634>.
- [RMPS23] ROMERO CALLA, LUCIANO ARNALDO, MOHANTO, BIPUL, PAJAROLA, RENATO, and STAADT, OLIVER. “Multi-Display Ray Tracing Framework”. *Eurographics 2023 - Posters*. Ed. by SINGH, GURPRIT and CHU, MENGJU (RACHEL). The Eurographics Association, 2023. ISBN: 978-3-03868-211-0. DOI: [10.2312/egp.2023102523](https://doi.org/10.2312/egp.2023102523).
- [RWH*17] ROTH, THORSTEN, WEIER, MARTIN, HINKENJANN, ANDRÉ, et al. “An analysis of eye-tracking data in foveated ray tracing”. Cited by: 12. 2017, 69–73. DOI: [10.1109/ETVIS.2016.7851170](https://doi.org/10.1109/ETVIS.2016.7851170). URL: <https://www.scopus.com/inward/record.uri?eid=2-s2.0-85015997302&doi=10.1109%2fETVIS.2016.7851170&partnerID=40&md5=e74b98273c37d0a91f09634b3edf30e44>.
- [RWM*15] ROTH, THORSTEN, WEIER, MARTIN, MAIERO, JENS, et al. “Guided High-Quality Rendering”. *Advances in Visual Computing*. Ed. by BEBIS, GEORGE, BOYLE, RICHARD, PARVIN, BAHRAM, et al. Cham: Springer International Publishing, 2015, 115–125. ISBN: 978-3-319-27863-6 2, 3.
- [SbMMS12] SALIH, YASIR, bt. MD-ESA, WAZIRAH, MALIK, AAMIR S., and SAAD, NAUFAL. “Tone mapping of HDR images: A review”. *2012 4th International Conference on Intelligent and Advanced Systems (ICIAS2012)*. Vol. 1. 2012, 368–373. DOI: [10.1109/ICTAS.2012.63062205](https://doi.org/10.1109/ICTAS.2012.63062205).
- [SCM15] SWAFFORD, NICHOLAS T., COSKER, DARREN, and MITCHELL, KENNY. “Latency Aware Foveated Rendering in Unreal Engine 4”. *Proceedings of the 12th European Conference on Visual Media Production*. CVMP '15. London, United Kingdom: Association for Computing Machinery, 2015. ISBN: 9781450335607. DOI: [10.1145/2824840.2824863](https://doi.org/10.1145/2824840.2824863). URL: <https://doi.org/10.1145/2824840.28248633>.
- [SCMP19] SIEKAWA, ADAM, CHWESIUK, MICHAŁ, MANTIUK, RADOŚŁAW, and PIÓRKOWSKI, RAFAŁ. “Foveated Ray Tracing for VR Headsets”. *MultiMedia Modeling*. Ed. by KOMPATSIARIS, IOANNIS, HUET, BENOIT, MEZARIS, VASILEIOS, et al. Cham: Springer International Publishing, 2019, 106–117. ISBN: 978-3-030-05710-7 2, 3.
- [SEB03] SHEIKH, HAMID R, EVANS, BRIAN L, and BOVIK, ALAN C. “Real-time foveation techniques for low bit rate video coding”. *Real-Time Imaging* 9.1 (2003), 27–40. ISSN: 1077-2014. DOI: [https://doi.org/10.1016/S1077-2014\(02\)00116-X](https://doi.org/10.1016/S1077-2014(02)00116-X). URL: <https://www.sciencedirect.com/science/article/pii/S107720140200116X3>.
- [SHL*23] SINGH, RAHUL, HUZAIFA, MUHAMMAD, LIU, JEFFREY, et al. “Power, Performance, and Image Quality Tradeoffs in Foveated Rendering”. *2023 IEEE Conference Virtual Reality and 3D User Interfaces (VR)*. 2023, 205–214. DOI: [10.1109/VR55154.2023.000362](https://doi.org/10.1109/VR55154.2023.000362).
- [TLZ*18] TAN, GUANJUN, LEE, YUN-HAN, ZHAN, TAO, et al. “Foveated imaging for near-eye displays”. *Opt. Express* 26.19 (Sept. 2018), 25076–25085. DOI: [10.1364/OE.26.025076](https://doi.org/10.1364/OE.26.025076). URL: <https://opg.optica.org/oe/abstract.cfm?URI=oe-26-19-250762>.
- [Vea98] VEACH, ERIC. “Robust Monte Carlo Methods for Light Transport Simulation”. AAI9837162. PhD thesis. Stanford, CA, USA, 1998. ISBN: 0591907801 5.

- [VKI*18] VIITANEN, TIMO, KOSKELA, MATIAS, IMMONEN, KALLE, et al. “Sparse sampling for real-time ray tracing”. English. *VISI-GRAPP 2018 - Proceedings of the 13th International Joint Conference on Computer Vision, Imaging and Computer Graphics Theory and Applications*. Vol. 1. INTERNATIONAL CONFERENCE ON COMPUTER GRAPHICS THEORY AND APPLICATIONS ; Conference date: 01-01-1900. SCITEPRESS, 2018, 295–302. DOI: [10 . 5220 / 0006655802950302 3](https://doi.org/10.5220/00066558029503023).
- [WAF*21] WALTON, DAVID R., ANJOS, RAFAEL KUFFNER DOS, FRISTON, SEBASTIAN, et al. “Beyond Blur: Real-Time Ventral Metamers for Foveated Rendering”. *ACM Trans. Graph.* 40.4 (July 2021). ISSN: 0730-0301. DOI: [10 . 1145 / 3450626 . 3459943](https://doi.org/10.1145/3450626.3459943). URL: <https://doi.org/10.1145/3450626.3459943>.
- [Wei19] WEIER, M. “Perception-driven rendering : techniques for the efficient visualization of 3D scenes including view- and gaze-contingent approaches”. (2019). Cited by: 1, 248. URL: <https://www.scopus.com/inward/record.uri?eid=2-s2.0-85118569502&partnerID=40&md5=9070d4f26189a7891a1ebaa35bd380382>.
- [Whi05] WHITTED, TURNER. “An improved illumination model for shaded display”. *ACM Siggraph 2005 Courses*. 2005, 4–es 3.
- [WMR*14] WEIER, MARTIN, MAIERO, JENS, ROTH, THORSTEN, et al. “Lazy Details for Large High-Resolution Displays”. *SIGGRAPH Asia 2014 Posters*. SA '14. Shenzhen, China: Association for Computing Machinery, 2014. ISBN: 9781450327923. DOI: [10 . 1145 / 2668975 . 2669016](https://doi.org/10.1145/2668975.2669016). URL: <https://doi.org/10.1145/2668975.2669016>.
- [WRK*16] WEIER, MARTIN, ROTH, THORSTEN, KRUIJFF, ERNST, et al. “Foveated Real-Time Ray Tracing for Head-Mounted Displays”. *Comput. Graph. Forum* 35.7 (Oct. 2016), 289–298. ISSN: 0167-7055 3, 4, 8.
- [WS19] WEI, LINGJIE and SAKAMOTO, YUJI. “Fast calculation method with foveated rendering for computer-generated holograms using an angle-changeable ray-tracing method”. *Appl. Opt.* 58.5 (Feb. 2019), A258–A266. DOI: [10 . 1364 / AO . 58 . 00A258](https://doi.org/10.1364/AO.58.00A258). URL: <https://opg.optica.org/ao/abstract.cfm?URI=ao-58-5-A2582>.
- [WSL23] WANG, LILI, SHI, XUEHUAI, and LIU, YI. “Foveated rendering: A state-of-the-art survey”. *Computational Visual Media* 9.2 (2023), 195–228. DOI: [10 . 1007 / s41095 - 022 - 0306 - 4](https://doi.org/10.1007/s41095-022-0306-4). URL: <https://www.sciopen.com/article/10.1007/s41095-022-0306-4>.
- [WSR*17] WEIER, M., STENGEL, M., ROTH, T., et al. “Perception-driven Accelerated Rendering”. *Computer Graphics Forum* 36.2 (2017), 611–643. DOI: <https://doi.org/10.1111/cgf.13150>. eprint: <https://onlinelibrary.wiley.com/doi/pdf/10.1111/cgf.13150>. URL: <https://onlinelibrary.wiley.com/doi/abs/10.1111/cgf.13150>.
- [YLC20] YANG, JINYUAN, LI, XIAOLI, and CAMPBELL, ABRAHAM G. “Variable Rate Ray Tracing for Virtual Reality”. *SIGGRAPH Asia 2020 Posters*. SA '20. Virtual Event, Republic of Korea: Association for Computing Machinery, 2020. ISBN: 9781450381130. DOI: [10 . 1145 / 3415264 . 3425451](https://doi.org/10.1145/3415264.3425451). URL: <https://doi.org/10.1145/3415264.3425451> 3, 4, 8.